

THE ARNOUX–YOCOZ MAPPING CLASSES VIA PENNER’S CONSTRUCTION

LIVIO LIECHTI AND BALÁZS STRENNER

ABSTRACT. We give a new description of the Arnoux–Yoccoz mapping classes as a product of two Dehn twists and a finite order element. The construction is analogous to Penner’s construction of mapping classes with small stretch factors.

1. INTRODUCTION

The mapping class group of a surface S is the group of isotopy classes of orientation-preserving homeomorphisms of S . Motivated by studying geometric structures on 3-manifolds, Thurston [Thu88] modernized the theory of mapping class groups in the 1970s by giving a classification of elements into three types: finite order, reducible and pseudo-Anosov. This article is concerned about the third type. A mapping class is *pseudo-Anosov* if it has a representative homeomorphism ϕ and singular measured foliations \mathcal{F}^u and \mathcal{F}^s on S such that $\phi(\mathcal{F}^u) = \lambda\mathcal{F}^u$ and $\phi(\mathcal{F}^s) = \lambda^{-1}\mathcal{F}^s$ for some $\lambda > 1$. The number λ is independent of choice of the representative homeomorphism and it is called the *stretch factor* or *dilatation* of the pseudo-Anosov mapping class.

Thurston showed that stretch factors of pseudo-Anosov mapping classes of the closed orientable surface S_g are algebraic integers with degree bounded above by $6g - 6$. He claimed without proof in [Thu88] that the degree $6g - 6$ was realizable, but this statement was only recently proven in [Str17]. For some time, however, even the fact that pseudo-Anosov stretch factors of arbitrarily large degrees exist was not justified. This fact was first shown by Arnoux and Yoccoz [AY81] in 1981. They constructed a pseudo-Anosov mapping class \tilde{h}_g on S_g for each $g \geq 3$ with a stretch factor of algebraic degree g . We will recall the construction in Section 2.1 and give more reasons for why the Arnoux–Yoccoz examples are of importance after stating the main results.

Despite the mapping classes \tilde{h}_g being probably the single most widely studied explicit family of pseudo-Anosov mapping classes, to this day, no constructions were known other than the original approach by Arnoux and Yoccoz.

The goal of the paper is to present a new description as a product of two Dehn twists and a finite order mapping class. We hope that this new description will shed new light on the examples and help construct new analogous families of mapping classes that might also serve as interesting

The first author was supported by the Swiss National Science Foundation (grant nr. 175260).

examples. An alternative description of the Arnoux–Yoccoz mapping classes was also asked for by Margalit in Section 10 of [Mar19].

Theorem 1.1. *The Arnoux–Yoccoz mapping class \tilde{h}_g on the surface S_g is conjugate to $\tilde{f}_g = r \circ T_a \circ T_b^{-1}$, where T_a and T_b^{-1} are positive and negative Dehn twists about the curves a and b pictured on Figure 1, and r is a rotation of the surface by one click in either direction.*

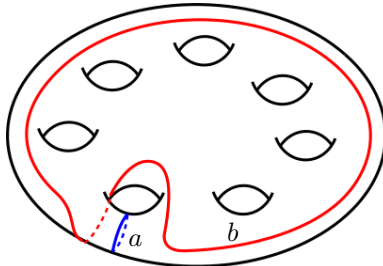


FIGURE 1. The surface S_g with a rotational symmetry of order g . This figure shows the case $g = 7$.

For the proof, we use the fact, shown by the second author in [Str18, Section 5], that the mapping classes \tilde{h}_g arise as lifts of mapping classes on nonorientable surfaces. More precisely, there is a pseudo-Anosov mapping class h_g (see Section 2.2 for the definition) on the closed nonorientable surface N_{g+1} of genus $g + 1$ for each $g \geq 3$ such that \tilde{h}_g is the lift of h_g by the double cover $S_g \rightarrow N_{g+1}$. We will deduce Theorem 1.1 from the following.

Theorem 1.2. *The nonorientable Arnoux–Yoccoz mapping class h_g on the surface N_{g+1} is conjugate to $f_g = r \circ T_c$, where T_c is a Dehn twist about the two-sided curve c pictured on Figure 2, and r is a rotation of the surface by one click in either direction.*

The direction of twisting about T_c is important, see Figure 6 later for the reason behind this. On a nonorientable surface, there is no notion of positive or negative twisting, so we specify the direction of the Dehn twist T_c by the coloring of the curve c on Figure 2 as follows. By cutting out the crosscap in the middle and cutting the twisted bands, we obtain an orientable surface with an embedding in \mathbf{R}^2 coming from the figure. Our cut-up surface inherits the orientation of \mathbf{R}^2 . The blue and red parts of our curve indicate the parts where the twisting behaves like a positive and negative twist, respectively, with respect to the orientation of the cut-up surface.

In Proposition 2.3 we show that both f_g^g and \tilde{f}_g^g arise from Penner’s construction. In this sense, the mapping classes f_g and \tilde{f}_g are analogous to the pseudo-Anosov mapping classes with small stretch factors constructed by Penner in [Pen91].

History and motivation. The Sah–Arnoux–Fathi invariant (in short, SAF invariant) is an invariant of interval exchange transformations and measured foliations that measures certain dynamical properties. In genus 2, the invariant foliations of all pseudo-Anosov mapping classes have non-vanishing

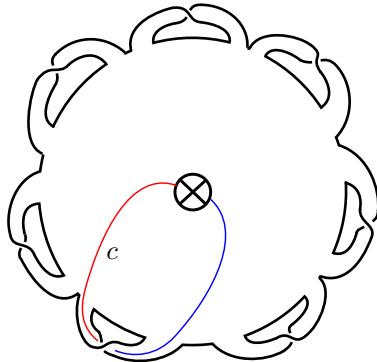


FIGURE 2. The circle with an X inside it indicates a crosscap: the inside of the circle is not part of the surface and antipodal points of the circle are identified. A disk with one crosscap is therefore a Möbius strip. So this figure shows a nonorientable surface obtained by attaching g twisted bands to the boundary of a Möbius strip. The surface has one boundary component. By gluing a disk to the boundary component, we obtain the closed surface N_{g+1} .

SAF invariant [McM03, Cal04]. The Arnoux–Yoccoz examples were the first examples for pseudo-Anosov mapping classes in genus 3 and higher whose invariant foliations had vanishing SAF invariants. For more on pseudo-Anosov maps with vanishing SAF invariant, see [AS09, CS13, DS16, Str18].

The Arnoux–Yoccoz examples are interesting also because they are known not to arise from Thurston’s construction [Thu88], the first general construction of pseudo-Anosov mapping classes. This was shown by Hubert and Lanneau [HL06], using the fact that the extension fields $\mathbf{Q}(\lambda_g + \lambda_g^{-1})$ are not totally real, where λ_g denotes the stretch factor of \tilde{h}_g . Since the examples that arise from Thurston’s construction have certain special properties (for one, see the next paragraph), the Arnoux–Yoccoz mapping classes have become valuable exotic examples.

A further motivation for studying the Arnoux–Yoccoz examples comes from Teichmüller theory. The two invariant measured foliations of a pseudo-Anosov mapping class give rise to a *singular Euclidean metric* or *flat structure* on the surface. The *Veech group* of a flat surface is the group of its affine symmetries. The infinite cyclic group formed by the powers of the pseudo-Anosov map is always part of the Veech group. It is not known, however, whether the Veech group can possibly equal this infinite cyclic group [HMSZ06, Problem 6]. In many cases (for example, for pseudo-Anosov maps arising from Thurston’s construction), the Veech group is known to contain free groups, hence it is known not to be cyclic. Since the Arnoux–Yoccoz examples do not arise from Thurston’s construction, presumably they might be good candidates for cyclic Veech groups. In the $g = 3$ case, however, Hubert, Lanneau and Möller [HLM09] found additional elements in the the Veech group of the Arnoux–Yoccoz flat surface, hence that Veech group is not cyclic. It remains an open question whether the Arnoux–Yoccoz surfaces have cyclic Veech groups when $g \geq 4$.

For other work on the Arnoux–Yoccoz mapping classes and their flat surfaces, see [Arn88, Bow10, Bow13, McM15, HW18].

Generalizations. The Arnoux–Yoccoz example in the $g = 3$ case has been generalized by Arnoux and Rauzy in Section 3 of [AR91], see also Section 4.2 of [PLV08]. On the surface N_4 , one example in the Arnoux–Rauzy family is the third power of the Arnoux–Yoccoz mapping class h_3 , which is conjugate to $T_{r-2(c)} \circ T_{r-1(c)} \circ T_c$ by our Theorem 1.2. We believe that other members of Arnoux–Rauzy family include the mapping classes $T_{r-2(c)} \circ T_{r-1(c)} \circ T_c^k$ where $k \geq 1$, but we will not give a proof of this.

In a follow-up paper [LS20], we will generalize the twist-and-rotation construction in Theorem 1.2 in a different way in order to construct minimal pseudo-Anosov stretch factors on various different nonorientable surfaces. In particular, we will show that the Arnoux–Yoccoz example h_3 has minimal stretch factor on N_4 among pseudo-Anosov mapping classes with an orientable invariant foliation.

Acknowledgements. We are grateful to Pierre Arnoux, Dan Margalit and Thomas Schmidt for helpful comments on an earlier version of this paper. We also thank the referees for their constructive feedback.

2. BACKGROUND

2.1. The orientable Arnoux–Yoccoz examples. In this section we recall the original construction of the orientable Arnoux–Yoccoz mapping classes \tilde{h}_g from [AY81]. We give this description in order to provide context only. The content of this section will not be used in the proofs.

Fix some $g \geq 3$ and let α be the unique real number in $(0, 1)$ satisfying $\alpha + \dots + \alpha^g = 1$. We construct a measured foliation \mathcal{F} on the surface S_g as follows. Start with the rectangle on Figure 3 foliated by vertical leaves. Equip \mathcal{F} with a measure so that the width of the rectangle is 2. Identify the two vertical sides to obtain a foliated annulus. Divide the top and bottom boundary components of this annulus to $2g$ intervals each as shown on Figure 3 and identify each interval on the top side with the interval on the bottom side that has the same length so that shaded rectangles above the core of the annulus are joined to shaded rectangles below the core of the annulus and empty rectangles are joined to empty rectangles. We obtain a measured foliation \mathcal{F} on the surface S_g . The two-sided simple closed curve γ obtained from the core of the annulus is transverse to \mathcal{F} and the first return map of \mathcal{F} with respect to γ induces the subdivision of S_g into the $2g$ rectangles shown on Figure 3.

The key observation is that the two-sided simple closed curve γ' on Figure 3 is also transverse to \mathcal{F} , has length 2α and the first return map of \mathcal{F} induces a decomposition into rectangles which is isomorphic to the original decomposition, up to scaling the measure by a factor of α . Therefore there are homeomorphisms of the surface that map γ to γ' and \mathcal{F} to $\frac{1}{\alpha}\mathcal{F}$. These homeomorphisms are all isotopic via a leaf-preserving isotopy, therefore they belong to the same mapping class. The mapping class \tilde{h}_g is defined to be this mapping class.

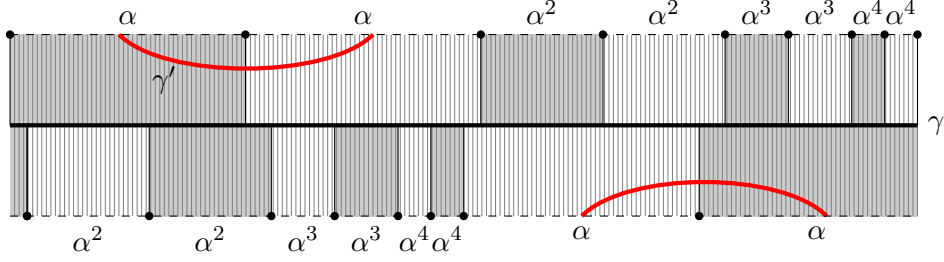


FIGURE 3. Construction of the mapping class \tilde{h}_4 by Arnoux and Yoccoz.

2.2. The nonorientable Arnoux–Yoccoz examples. In [Str18], the second author has constructed a mapping class h_g on the closed nonorientable surface N_{g+1} of genus $g + 1$ in a way that is analogous to the construction described in Section 2.1.

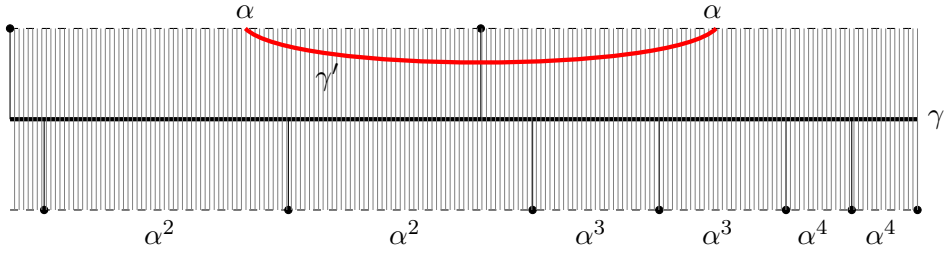


FIGURE 4. Construction of the mapping class h_4 by the second author.

Consider the rectangle on Figure 4 together with the vertical measured foliation of width 1, but now identify the two vertical sides with a flip to obtain a foliated Möbius strip. Divide the boundary component of length 2 to intervals as shown on the figure and identify pairs of intervals of equal length by translations.

Let γ be the core of the Möbius strip and let γ' be the one-sided curve in the figure that is also transverse to the foliation \mathcal{F} . As before, the first return maps of the foliation on γ and γ' each induce decompositions of the surface into g foliated rectangles, and there are homeomorphisms that map γ to γ' and \mathcal{F} to $\frac{1}{\alpha}\mathcal{F}$. Once again, all these homeomorphisms are isotopic hence they define the same mapping class. The mapping class h_g is defined to be this mapping class.

Our approach for proving that a mapping class constructed in a different way is conjugate to h_g is to use the fact (immediate from the construction) that the triple $(\mathcal{F}, \gamma, \gamma')$ uniquely determines h_g up to conjugation. To be more specific, we state this fact formally as follows.

Lemma 2.1. *Let $g \geq 3$ and let f_1 and $f_2 = h_g$ be pseudo-Anosov mapping classes with unstable measured foliations \mathcal{F}_1 and \mathcal{F}_2 on the surface N_{g+1} . Let γ_1 and γ_2 be one-sided simple closed curves on N_{g+1} , transverse to \mathcal{F}_1 and \mathcal{F}_2 , respectively. If there is a homeomorphism $\phi : N_{g+1} \rightarrow N_{g+1}$ such*

that $\phi(\mathcal{F}_1) = \mathcal{F}_2$, $\phi(\gamma_1) = \gamma_2$ and $\phi(f_1(\gamma_1)) = f_2(\gamma_2)$, then f_1 and f_2 are conjugate in the mapping class group of N_{g+1} .

2.3. Penner's construction of pseudo-Anosov mapping classes. Consider the annulus $A = \{z \in \mathbf{C} : 1 \leq |z| \leq 2\}$ and define the positive Dehn twist in A by the formula $T(z) = z \cdot e^{2\pi i(1-|z|)}$. Given a two-sided simple closed curve c in a surface S , its *marking* is an embedding $\phi_c : A \rightarrow S$ where c is the image of the circle $\{z : |z| = \frac{3}{2}\}$. The Dehn twist about the marked curve (c, ϕ_c) is defined as $\phi_c \circ T \circ \phi_c^{-1}$ on $\phi_c(A)$ and as the identity otherwise. When the marking is clear from the context, we denote this Dehn twist simply by T_c . Note that if the surface S is orientable, then T_c is a positive twist if ϕ_c is orientation-preserving and a negative twist if ϕ_c is orientation-reversing.

Two marked two-sided simple closed curves c_1 and c_2 are said to *intersect inconsistently* if $\phi_{c_1}^{-1} \circ \phi_{c_2}$ is orientation-reversing at all points where the composition is defined. A pair of simple closed curves on a surface is in *minimal position* if one cannot decrease their intersection number by isotoping them. A collection of curves on a surface is said to *fill* the surface if they are in pairwise minimal position and the complementary regions of the curves are disks and once-punctured disks.

Penner gave the following construction of pseudo-Anosov mapping classes in [Pen88] (see also [Fat92]).

Theorem 2.2 (Penner's construction). *Let c_1, \dots, c_n be a filling collection of pairwise inconsistently intersecting marked two-sided simple closed curves on a surface S . Then any product of the Dehn twists T_{c_1}, \dots, T_{c_n} containing each twist at least once is pseudo-Anosov.*

For an orientable surface, the filling and the inconsistently intersecting property implies that the collection of curves is a union of two multicurves Γ_1 and Γ_2 and the allowable products contain positive twists about the curves in Γ_1 and negative twists about the curves in Γ_2 .

One nice property of Penner's construction is that the stretch factor and the invariant measured foliations are straightforward to compute. We explain the process briefly here, for more details, see [Pen88, Pen91, Fat92, Str17]. By smoothing out the intersections of the collection $\{c_1, \dots, c_n\}$, one obtains a bigon track τ that is invariant under each twist T_{c_i} , hence under any product of them as well. This process is illustrated on Figure 5. Each curve c_i is carried on τ and its characteristic measure μ_i is a 0-1-valued measure on τ that takes the value 1 on the branches of τ traversed by c_i and the value 0 on the other branches. The cone C generated by the measures μ_i is invariant under the Dehn twists T_{c_i} . Moreover, a product f of T_{c_i} containing all twists at least once acts on C by a Perron–Frobenius matrix (a matrix with nonnegative entries that has a power whose entries are all positive). The largest eigenvalue of this matrix has multiplicity 1 and it is the stretch factor of f . The corresponding eigenvectors define a positive measure on τ that is unique up to scaling, and this train track measure defines the unstable foliation of f .

Proposition 2.3. *The mapping classes f_g^g and \tilde{f}_g^g arise from Penner's construction.*

Proof. We have

$$f_g^g = T_{r^{-(g-1)}(c)} \circ \cdots \circ T_c.$$

and

$$\tilde{f}_g^g = T_{r^{-(g-1)}(a)} \circ T_{r^{-(g-1)}(b)}^{-1} \circ \cdots \circ T_a \circ T_b^{-1}.$$

Figure 5A shows that the marked curve c and its rotated copies intersect inconsistently (red intersects blue at every intersection). Furthermore, any pair of curves intersects exactly once and hence minimally, and the complement of the union of the curves consists of discs. Hence f_g^g indeed arises from Penner’s construction.

In the second case, $A = \{a, \dots, r^{g-1}(a)\}$ and $B = \{b, \dots, r^{g-1}(b)\}$ are filling multicurves, and we twist only positively along curves in A and negatively along curves in B , hence \tilde{f}_g^g also arises from Penner’s construction. \square

3. PROOFS

In this section, we give the proofs of Theorem 1.1 and Theorem 1.2.

Proof of Theorem 1.2. By Lemma 2.1, the proof reduces to the study of the unstable foliation of f_g and the image of the core curve γ of the crosscap under f_g .

First we describe the unstable foliation of f_g . Although f_g does not arise from Penner’s construction, its g th power does, since

$$f_g^g = T_{r^{-(g-1)}(c)} \circ \cdots \circ T_c.$$

The invariant foliations of f_g and its powers are the same, therefore we may use the process described in Section 2.3 for f_g^g to find the unstable foliation of f_g .

Figure 5A shows the curve c and its iterates under the rotation r and Figure 5B shows the invariant bigon track of f_g^g obtained by smoothing out the intersections of these curves. Note that this bigon track is invariant not only under all twists $T_{r^i(c)}$, but also under r .

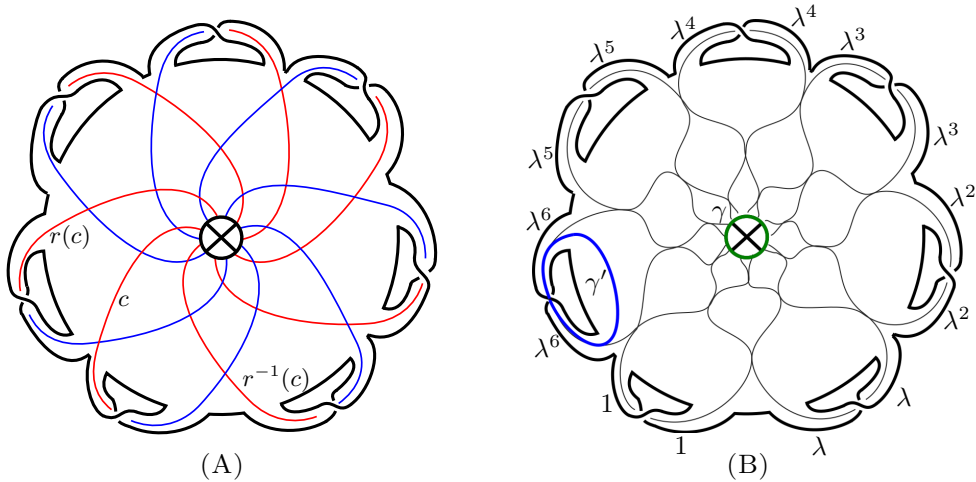


FIGURE 5

For $i = 0, \dots, g-1$, let μ_i be the characteristic measure of the curve $r^{-i}(c)$. The mapping class T_c acts on the cone C generated by the characteristic measures μ_i by the matrix which has 1s on the diagonal and in the first row, and 0s otherwise, and r acts by a permutation matrix. So, for example, when $g = 7$, the acting matrix of $f_g = r \circ T_c$ on the cone C is

$$M_g = \begin{pmatrix} 0 & 1 & 0 & 0 & 0 & 0 & 0 \\ 0 & 0 & 1 & 0 & 0 & 0 & 0 \\ 0 & 0 & 0 & 1 & 0 & 0 & 0 \\ 0 & 0 & 0 & 0 & 1 & 0 & 0 \\ 0 & 0 & 0 & 0 & 0 & 1 & 0 \\ 0 & 0 & 0 & 0 & 0 & 0 & 1 \\ 1 & 1 & 1 & 1 & 1 & 1 & 1 \end{pmatrix},$$

the companion matrix of the polynomial $x^7 - x^6 - \dots - x - 1$. In general, the characteristic polynomial is $x^g - x^{g-1} - \dots - x - 1$. The action of f_g^g on C is given by M_g^g , so by the construction described in Section 2.3, the stretch factor and the unstable foliation of f_g^g are the largest eigenvalue and the corresponding eigenvector for M_g^g . As a consequence, the stretch factor and the unstable foliation of f_g are given by the largest eigenvalue and the corresponding eigenvector for M_g . Hence the stretch factor λ of f_g is the largest real root of $x^g - x^{g-1} - \dots - x - 1$. The corresponding eigenvector is $(1, \lambda, \lambda^2, \dots, \lambda^{g-1})$, therefore the unstable foliation of f_g is given by the measure $\sum_{i=0}^{g-1} \lambda^i \mu_i$ on our bigon track. Note that $\lambda = 1/\alpha$ where α was defined in Section 2.1.

Now we explain how to redraw Figure 5B analogously to Figure 4. (Note, however, that Figure 5B depicts the case $g = 7$, while Figure 4 shows the case $g = 4$.) A large regular neighborhood of γ on Figure 5B is the disk with the crosscap in the middle (hence a Möbius strip), but without the twisted bands attached. Since a bigon in the complement of a bigon track does not give rise to a singularity of the unstable measured foliation, we can isotope the foliation so that its leaves point radially inwards from the boundary of the Möbius strip, and so that the foliation is nonsingular in the interior of the Möbius strip. Note that, up to homeomorphism preserving the leaves and the transverse measure of the foliation, every nonsingular measured foliation of the Möbius strip whose leaves meet the boundary transversally is the vertical foliation of a rectangle with the two vertical sides identified by an involution. This is the model of Figure 4, but without the identifications on the boundary. Therefore, the only thing left to check is that attaching the twisted bands as in Figure 5B induces the correct identifications of the boundary in the Möbius rectangle model.

The effect of attaching the twisted bands is that intervals on the boundary of the Möbius strip get identified. The lengths of these intervals with respect to the unstable measured foliation are the measures on the branches of the bigon track inside the twisted bands, that is, $\lambda^{g-1}, \lambda^{g-1}, \dots, 1, 1$. When the Möbius strip is drawn as a rectangle with its vertical sides identified, the $2g$ intervals of length $\lambda^{g-1}, \lambda^{g-1}, \dots, 1, 1$ appear on the horizontal sides. Note that we obtain exactly the pattern of Figure 4, with the difference that our intervals are a factor λ^g longer. Since the bands on Figure 5B are twisted,

the pairs of intervals are glued together in an orientation-reversing way, just like gluing by translation on Figure 4 results in orientation-reversing gluings. Therefore the bigon track on Figure 5B indeed produces the measured foliation pictured on Figure 4, up to scaling the measure by λ^g .

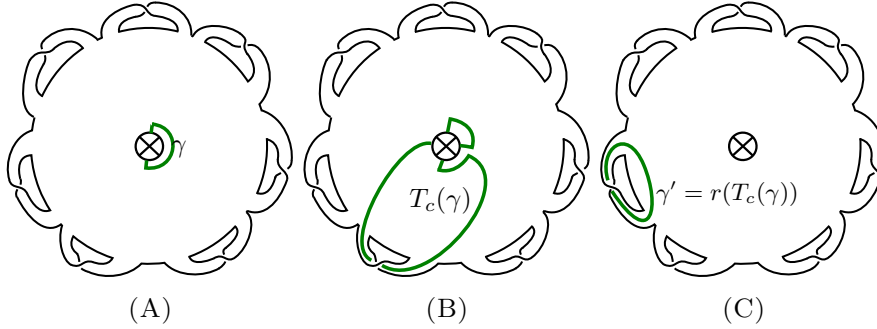


FIGURE 6. The curves γ , $T_c(\gamma)$, and $\gamma' = r(T_c(\gamma))$. To go from the second figure to the third, we isotope a small piece of $T_c(\gamma)$ through the crosscap. This is possible, because the antipodal points of the circle containing the X are identified. The direction of the twisting about c matters: one can compute directly that the curve $T_c^{-1}(\gamma)$ defines an element of the fundamental group that does not correspond to the core curve of one of the twisted bands.

The curve $\gamma' = h_g(\gamma)$ on Figure 4 corresponds to the curve γ' on Figure 5B. It remains to show that $\gamma' = f_g(\gamma)$. After applying the twist T_c on the curve γ on Figure 6A, we obtain the curve shown on Figure 6B. After rotation by one click, this curve indeed maps to γ' . \square

Proof of Theorem 1.1. Consider the orientable double cover of the nonorientable surface in Figure 2. One way to construct this covering surface is to cut along the twisted bands on Figure 5B, remove the central crosscap, and glue together two copies of the resulting surface. We can think about the two copies as the upper and lower half of the cylinder pictured on Figure 7. The upper and lower boundaries of this cylinder are subdivided into $2g$ intervals, which correspond to the $2g$ intervals obtained by cutting the twisted bands. The orientation-reversing involution of this cylinder that

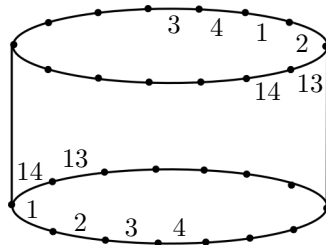


FIGURE 7. The orientable double cover of the surface on Figure 2 when $g = 7$.

identifies the upper and lower half is the reflection about the center of the

picture in the ambient 3-dimensional space. When the intervals along the boundaries are identified in the manner shown, the quotient of the surface is our nonorientable surface with the twisted bands, with the boundary collapsed to one point.

Note that the rotation r of N_{g+1} lifts to the rotation of the cylinder by two intervals.

By flattening out the cylinder, we obtain the representation on Figure 8A. The lift of the curve c along which we twist in the definition of f_g has two

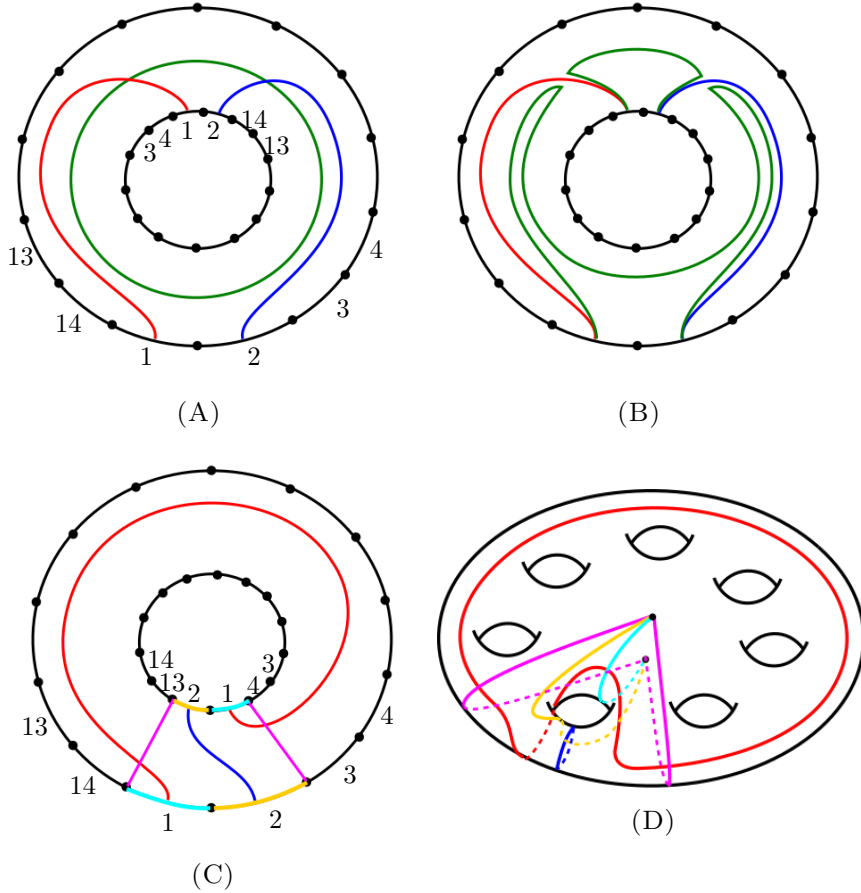


FIGURE 8

components, shown on Figure 8A. A Dehn twist about the curve c on N_{g+1} lifts to the product of a positive twist along one of the lifts of c and a negative twist about the other lift.

To find out which twist is positive and which twist is negative, recall that $T_c(\gamma)$ is a curve that runs in a small neighborhood of one of the twisted bands (Figures 6A and 6B). The core curve of the annulus on Figure 8A is the lift of γ , so its image under the two twists should run in a small neighborhood of two consecutive intervals of the boundary of the annulus. That happens when the twist is positive along the curve on the right and negative along the curve on the left on Figure 8B.

After changing Figure 8A by rotating the inner boundary by 180 degrees, we obtain the representation shown on Figure 8C. By subdividing this surface along the arcs shown and their rotated copies, we can see that this surface can be represented in \mathbf{R}^3 as the surface on Figure 8D. The two twisting curves correspond to the curves shown on Figure 1, and we indeed twist positively along the curve a and negatively along the curve b . \square

Remarks on the order of composition and the direction of twisting. Recall from Theorem 1.1 the definition of the curves a and b and the rotation r . Consider also the curve b' on Figure 9 that winds around the hole to avoid a in the direction opposite of b .

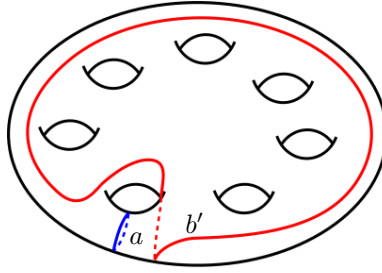


FIGURE 9

The following statement summarizes the ways in which the definition of the mapping class $\tilde{f}_g = r \circ T_a \circ T_b^{-1}$ is flexible.

Proposition 3.1. *The following statements hold.*

- (1) T_a commutes with both T_b^{-1} and $T_{b'}^{-1}$.
- (2) \tilde{f}_g is conjugate to $r^{\pm 1} \circ T_a \circ T_b^{-1}$, $T_a \circ T_b^{-1} \circ r^{\pm 1}$, $r^{\pm 1} \circ T_a^{-1} \circ T_{b'}$ and $T_a^{-1} \circ T_{b'} \circ r^{\pm 1}$.
- (3) \tilde{f}_g^{-1} is conjugate to $T_a^{-1} \circ T_b \circ r^{\pm 1}$, $r^{\pm 1} \circ T_a^{-1} \circ T_b$, $T_a \circ T_{b'}^{-1} \circ r^{\pm 1}$ and $r^{\pm 1} \circ T_a \circ T_{b'}^{-1}$.

Proof. The first statement holds, because a is disjoint from b and b' .

For the first expression in the second statement, note that on Figure 1, the rotation by 180 degrees about the axis intersecting a and b symmetrically commutes with both T_a and T_b^{-1} , but conjugates r to r^{-1} . The second expression is conjugate to the first by r . For the third and fourth expressions, note that the reflection about the plane that intersects all g holes of the surface commutes with r and conjugates T_a to T_a^{-1} and T_b to T_b^{-1} .

The third statement follows from the second by taking the inverse. \square

To summarize, the order of the two twists, the direction of the rotation and whether we twist first or rotate first do not matter.

In the nonorientable case, we have the following.

Proposition 3.2. *The mapping class f_g is conjugate to $r^{\pm 1} \circ T_c$ and $T_c \circ r^{\pm 1}$. The inverse f_g^{-1} is conjugate to $T_c^{-1} \circ r^{\pm 1}$ and $r^{\pm 1} \circ T_c^{-1}$.*

Proof. This follows by conjugating by r and by an involution of the surface that rotates about an axis and leaves the curve c invariant. This involution commutes with T_c and conjugates r to r^{-1} . \square

We also remark that it can be shown by studying their flat surfaces that h_g is conjugate to h_g^{-1} and \tilde{h}_g is conjugate to \tilde{h}_g^{-1} when $g = 3$, but not if $g > 3$. Therefore one indeed needs to be careful about the definitions, because the direction in which b winds around the hole does matter.

REFERENCES

- [AR91] Pierre Arnoux and Gérard Rauzy. Représentation géométrique de suites de complexité $2n + 1$. *Bull. Soc. Math. France*, 119(2):199–215, 1991.
- [Arn88] Pierre Arnoux. Un exemple de semi-conjugaison entre un échange d’intervalles et une translation sur le tore. *Bull. Soc. Math. France*, 116(4):489–500 (1989), 1988.
- [AS09] Pierre Arnoux and Thomas A. Schmidt. Veech surfaces with nonperiodic directions in the trace field. *J. Mod. Dyn.*, 3(4):611–629, 2009.
- [AY81] Pierre Arnoux and Jean-Christophe Yoccoz. Construction de difféomorphismes pseudo-Anosov. *C. R. Acad. Sci. Paris Sér. I Math.*, 292(1):75–78, 1981.
- [Bow10] Joshua P. Bowman. Orientation-reversing involutions of the genus 3 Arnoux-Yoccoz surface and related surfaces. In *In the tradition of Ahlfors-Bers. V*, volume 510 of *Contemp. Math.*, pages 13–23. Amer. Math. Soc., Providence, RI, 2010.
- [Bow13] Joshua P. Bowman. The complete family of Arnoux-Yoccoz surfaces. *Geom. Dedicata*, 164:113–130, 2013.
- [Cal04] Kariane Calta. Veech surfaces and complete periodicity in genus two. *J. Amer. Math. Soc.*, 17(4):871–908, 2004.
- [CS13] Kariane Calta and Thomas A. Schmidt. Infinitely many lattice surfaces with special pseudo-Anosov maps. *J. Mod. Dyn.*, 7(2):239–254, 2013.
- [DS16] Hieu Trung Do and Thomas A. Schmidt. New infinite families of pseudo-Anosov maps with vanishing Sah-Arnoux-Fathi invariant. *J. Mod. Dyn.*, 10:541–561, 2016.
- [Fat92] Albert Fathi. Démonstration d’un théorème de Penner sur la composition des twists de Dehn. *Bull. Soc. Math. France*, 120(4):467–484, 1992.
- [HL06] Pascal Hubert and Erwan Lanneau. Veech groups without parabolic elements. *Duke Math. J.*, 133(2):335–346, 2006.
- [HLM09] Pascal Hubert, Erwan Lanneau, and Martin Möller. The Arnoux-Yoccoz Teichmüller disc. *Geom. Funct. Anal.*, 18(6):1988–2016, 2009.
- [HMSZ06] Pascal Hubert, Howard Masur, Thomas Schmidt, and Anton Zorich. Problems on billiards, flat surfaces and translation surfaces. In *Problems on mapping class groups and related topics*, volume 74 of *Proc. Sympos. Pure Math.*, pages 233–243. Amer. Math. Soc., Providence, RI, 2006.
- [HW18] W. Patrick Hooper and Barak Weiss. Rel leaves of the Arnoux–Yoccoz surfaces. *Selecta Math. (N.S.)*, 24(2):875–934, 2018.
- [LS20] Livio Liehti and Balázs Strenner. Minimal pseudo-Anosov stretch factors on nonoriented surfaces. *Algebr. Geom. Topol.*, 20(1):451–485, 2020.
- [Mar19] Dan Margalit. Problems, questions, and conjectures about mapping class groups. *Proc. Sympos. Pure Math.*, 102:157–186, 2019.
- [McM03] Curtis T. McMullen. Teichmüller geodesics of infinite complexity. *Acta Math.*, 191(2):191–223, 2003.
- [McM15] Curtis T. McMullen. Cascades in the dynamics of measured foliations. *Ann. Sci. Éc. Norm. Supér. (4)*, 48(1):1–39, 2015.
- [Pen88] Robert C. Penner. A construction of pseudo-Anosov homeomorphisms. *Trans. Amer. Math. Soc.*, 310(1):179–197, 1988.
- [Pen91] Robert C. Penner. Bounds on least dilatations. *Proc. Amer. Math. Soc.*, 113(2):443–450, 1991.
- [PLV08] G. Poggiaspalla, J. H. Lowenstein, and F. Vivaldi. Geometric representation of interval exchange maps over algebraic number fields. *Nonlinearity*, 21(1):149–177, 2008.

- [Str17] Balázs Strenner. Algebraic degrees of pseudo-Anosov stretch factors. *Geom. Funct. Anal.*, 27(6):1497–1539, 2017.
- [Str18] Balázs Strenner. Lifts of pseudo-Anosov homeomorphisms of nonorientable surfaces have vanishing SAF invariant. *Math. Res. Lett.*, 25(2):677–685, 2018.
- [Thu88] William P. Thurston. On the geometry and dynamics of diffeomorphisms of surfaces. *Bull. Amer. Math. Soc. (N.S.)*, 19(2):417–431, 1988.

DÉPARTEMENT DE MATHÉMATIQUES, UNIVERSITÉ DE FRIBOURG, CHEMIN DU MUSÉE
23, 1700 FRIBOURG, SUISSE

Email address: `livio.liechti@unifr.ch`

GEORGIA INSTITUTE OF TECHNOLOGY, SCHOOL OF MATHEMATICS, ATLANTA GA
30332, USA

Email address: `strenner@math.gatech.edu`

Email address: `strennerb@gmail.com`